Computer-aided recognition of Discharge Sources

E. Gulski and F. H. Kreuger

HV Laboratory, Electrical Engineering Department,
Delft University of Technology, Delft, The
Netherlands

ABSTRACT

Making use of a computer-aided discharge analyzer, a combination of statistical and discharge parameters was studied to discriminate between different discharge sources. Tests on samples with different discharge sources revealed that several parameters are characteristic for different types of discharges and offer good discrimination between different defects.

1. INTRODUCTION

DISCHARGE detection is an important means of testing the reliability of HV cables, transformers, insulators, etc. Throughout the years, many successful methods for detection, location and evaluation of partial discharge (PD) phenomena have been developed for this purpose. However, the correlation found between the measured discharge magnitude and the discharge process that takes place inside the insulation is limited. Although several discharge quantities used today do not predict the lifetime of the dielectric, they do give information on its quality. PD measurement often provides a means for detecting defects that could lead to the breakdown of the dielectric [1].

As each defect has its own particular degradation mechanism, it is important to know the correlation between discharge patterns and the kind of defect. Therefore progress in the recognition of internal discharge and their correlation with the kind of defect is becoming increasingly important in the quality control in insulating systems [2]. One of the undoubted advantages of a computer-aided measuring system is the ability to process a large amount of information and to transform this information into an understandable output. Many computer-aided systems have been developed for the measurement and understanding of PD phenomena. In particular, the trend

is in the direction of improvement of the recognition of discharge sources and the evaluation of measuring results, which will assist in the judgment of the quality and the condition of insulating systems [3-6].

For PD analysis, more than twenty discharge quantities are at our disposal [7]. Therefore a computer-aided discharge analyzer has been built for continuous and multi-parameter recording [8]. In this study we will concentrate on a selected number of discharge quantities using the analyzer during short tests (20 min maximum). The following discharge sources were tested: single vs. multiple cavities, electrode-bounded vs. dielectric-bounded cavities, treeing initiated by a cavity, treeing initiated by a conductor, and surface discharges in air.

Our aim was to find a good discriminator between these discharge sources by studying the behavior of several statistical parameters.

2. PD QUANTITIES

TO describe the characteristics of a discharge, many discharge quantities have been introduced over the years [7]. With regard to the observation time, these quantities can be divided into three main groups.
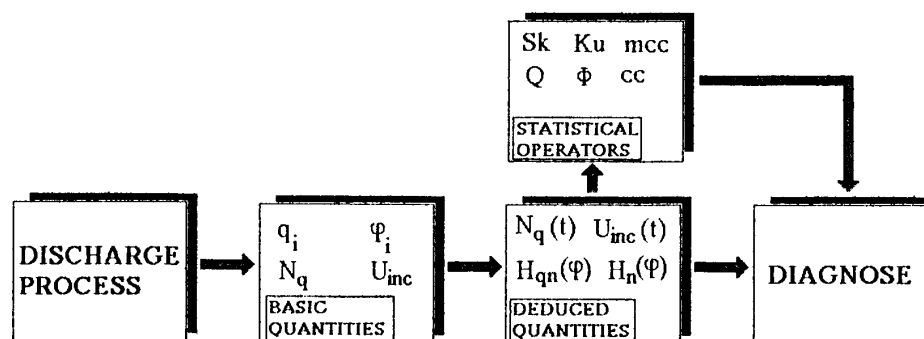
Figure 1.   Block diagram of discharge analysis.

1. Basic quantities, which are quantities observed during one voltage cycle.
2. Deduced quantities, which are integrated values of basic quantities from the first group observed throughout several voltage cycles.
3. Statistical operators, which are operators for the statistical analysis of the deduced parameters.

It is evident that each quantity can give partial information only. The analysis has shown that the observation of several discharge quantities will lead to a better evaluation [5,9]. Based on this supposition, a diagnostic system for discharge measurement has been developed. A computer-aided system is proposed for the systematic processing of the discharge quantities (Figure 1).
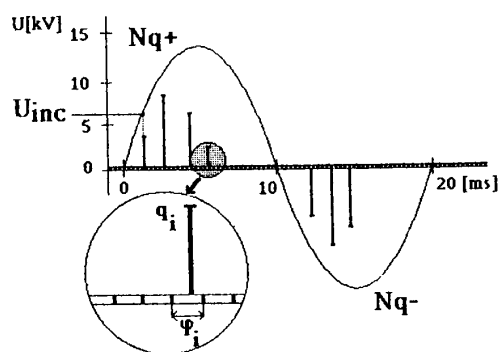

Figure 2.
Schematic diagram of discharge quantities.

2.1 BASIC QUANTITIES

For the registration of basic quantities, the momentary values of the test voltage and the discharge signal were processed. It is known that using conventional detection methods (bandwidth $\sim$ 400 kHz) the electrical activity of

PD is represented by three independent quantities only: the discharge magnitude q_i, the ignition voltage U_i and the position of the discharge related to the phase angle φ_i of the test voltage. If during one half cycle of the test voltage more discharges occur, on the basis of q_i, U_i and φ_i several quantities can be calculated [8]. For this study following basic quantities were measured and processed (Figure 2): the inception voltage U_{inc} as a voltage at the sample at which discharge pattern in a half cycle of the test voltage starts and the number of discharges for each halve period of the voltage cycle N_q.

2.2 DEDUCED QUANTITIES

For the registration of deduced quantities, the basic quantities have to be observed during a time span that is much longer than the duration of one voltage cycle, e.g. > 100 cycles. These quantities can be analyzed as a function of time and as a function of the phase angle.

The quantities as function of time describe the changes of the basic quantities in the course of time. It is known that statistical variation in PD occurs, both in magnitude and in the temporal behavior of discharges. This variation in the time is partly caused by statistical variations in the discharge phenomenon itself and it is partly the result of the changes in the discharge site. Therefore, to get the information on the conditions of the dielectric surfaces on a discharge site, the time behavior in the positive and negative half of the voltage cycle of inception voltage $U_{inc}(t)$ and the number of discharges $N_q(t)$ were processed. The quantities as function of the phase angle represent the recurrence of PD related to their phase angle. Therefore the voltage cycle was divided into phase windows representing the phase angle axis (0 to 360°) (Figure 2). If the observation takes place over several voltage cycles, four quantities can be determined in each

phase window: the sum of the discharge magnitudes, the number of discharges, the average value of discharges and the maximum value of discharges. These quantities, observed throughout the whole angle axis, result in distributions of discharge recurrence as a function of phase angle. By measuring pulse distributions as a function of the phase angle it is possible to obtain information on the phenomena that cause these distributions [5, 9–13]. For this study following phase-position quantities were processed [13]: the pulse count distribution $H_n(\varphi)$, which represents the number of observed discharges in each phase window as a function of the phase angle; and the mean pulse height distribution $H_{qn}(\varphi)$, which represents the average amplitude in each phase window as a function of the phase angle. $H_{qn}(\varphi)$ is derived from the total discharge amount in each phase window divided by the pulse number of discharges in the same phase window.

Generally, for the display of these phase-position quantities, a choice had to be made between a two-dimensional and a three-dimensional presentation. It is known that the combination of $H_{qn}(\varphi)$ and the $H_n(\varphi)$ quantities can be displayed as a three-dimensional distribution having the advantage of visible strength. However, because of its complexity, such a picture is more difficult to analyze quantitatively. Therefore, the choice was made to display and to analyze the $H_{qn}(\varphi)$ and the $H_n(\varphi)$ quantities separately as two-dimensional distributions.

According to several authors, the time dependence of the pulse count phase distribution $H_n(\varphi)$ and the mean pulse height distribution $H_{qn}(\varphi)$ provide a good description of changes in discharge patterns. The $H_n(\varphi)$ quantity in the course of time contains information of the intensity of discharges as a function of their inception phase angle. This allows the recognition of discharge sources and their behavior in time. The $H_{qn}(\varphi)$ quantity allows noise reduction due to the difference between the statistical characteristics of the discharge pulses and that of noise pulses as a function of phase angle [4, 5, 13].

In reality, we can say that the discharges occur during a voltage cycle in two sequences: for each half of the voltage cycle separate discharge patterns can be measured. But in the case of similar inception conditions for each half of the voltage cycle, equal discharge patterns can be expected. Therefore the $H_{qn}(\varphi)$ and $H_n(\varphi)$ quantities are characterized by two distributions: for the positive half of the voltage cycle $H_{qn}^+(\varphi)$, $H_n^+(\varphi)$ and for the negative half of the voltage cycle $H_{qn}^-(\varphi)$ and $H_{qn}^-(\varphi)$.

2.3 STATISTICAL OPERATORS

To study the differences between the distributions $H_{qn}^+(\varphi)$ and $H_{qn}^-(\varphi)$ in both halves of the voltage cycle

the following statistical operators have been introduced by the author [9]:

Discharge asymmetry

The discharge asymmetry Q is the quotient of the mean discharge level of the $H_{qn}(\varphi)$ distribution in the positive and in the negative half of voltage cycle

$$Q = \frac{Q_s^-/N^-}{Q_s^+/N^+} \qquad (1)$$

where Q_s^+ and Q_s^- are the sum of discharges of the $H_{qn}(\varphi)$ distribution in the positive and the negative half of the voltage cycle; N^+ and N^- are the number of discharges of the $H_{qn}(\varphi)$ distribution in the positive or negative half of the voltage cycle.

Phase asymmetry

The phase asymmetry Φ is used to study the difference in inception voltage of the $H_{qn}(\varphi)$ distribution in the positive and negative half of the voltage cycle:

$$\Phi = \frac{\varphi_{in}^-}{\varphi_{in}^+} \qquad (2)$$

where φ_{in}^+ and φ_{in}^- are the inception phase of the $H_{qn}(\varphi)$ distribution in the positive and the negative half of the voltage cycle.

Moreover, a factor is introduced which is known from the statistical literature.

The cross-correlation factor

The factor cc is used to evaluate the difference in shape of distributions $H_{qn}^+(\varphi)$ and $H_{qn}^-(\varphi)$. The following formula is used to calculate the cross-correlation factor

$$cc = \frac{\sum xy - \sum x \sum y/n}{\sqrt{[\sum x^2 - (\sum x)^2/n][\sum y^2 - (\sum y)^2/n]}} \qquad (3)$$

where x is the mean discharge magnitude in a phase window in the positive half of the voltage cycle; y the mean discharge magnitude in the corresponding phase window in the negative half of the voltage cycle; and n the number of phase positions per half cycle.

Thus, the differences between the distributions $H_{qn}^+(\varphi)$ and $H_{qn}^-(\varphi)$ are described by three independent parameters: phase asymmetry Φ, discharge asymmetry Q and cross-correlation factor cc. A cross correlation $cc = 1$ means a 100% shape symmetry and a value of 0 indicates total asymmetry. However, cc tells us nothing about the height of the distribution. For that purpose we use the

discharge asymmetry Q or phase asymmetry Φ. Both these variables are defined in such a way that they are equal to 1 in the case of fully symmetric distributions and smaller than one in the case of asymmetric ones. Thus several asymmetry factors can be easily combined (having equal weight) by multiplication. Therefore the operator mcc has been introduced by the author [9]

The modified cross-correlation factor

This factor mcc is used to evaluate the differences between discharge patterns in the positive and the negative voltage cycle. This is defined as the product of phase asymmetry Φ, discharge asymmetry Q and cross-correlation factor cc

$$mcc = \Phi \cdot Q \cdot cc \qquad (4)$$

It is known from the literature that in the case of a single defect, discharge parameters can be fairly well described by a normal distribution process. Therefore to get a better evaluation of $H_{qn}(\varphi)$ and $H_n(\varphi)$ quantities, several statistical parameters typical for normal distribution can be used. Here are named after the following statistical operators [14]

Skewness Sk

An indicator for the asymmetry of a distribution with respect to a normal distribution

$$Sk = \frac{\sum (x_i - \mu)^3 \cdot P_i}{\sigma^3} \qquad (5)$$

Kurtosis Ku

The indicator for the deviation from the normal distribution

$$Ku = \frac{\sum (x_i - \mu)^4 \cdot P_i}{\sigma^4} - 3 \qquad (6)$$

where x_i is the discrete value; P_i the probability for x_i; μ the mean value of the distribution; and σ the standard deviation of the distribution.

These statistical operators are significant in connection with the shape of the distribution. They can therefore be used to characterize the distribution functions $H_{qn}(\varphi)$ and $H_n(\varphi)$ more precisely [15]. The skewness Sk indicates the asymmetry of the distribution and Sk is zero for a symmetric distribution, positive when the distribution is asymmetric to the left, and negative when the distribution is asymmetric to the right (Figure 3). The kurtosis Ku indicates the sharpness of the distribution and Ku is zero for a normal distribution. For a sharper

than normal distribution Ku is positive, and if the distribution is flatter than the normal distribution the Ku is negative (Figure 3).

3. EXPERIMENTAL WORK

To investigate whether typical sources of discharges in solids can be recognized by a specific discharge pattern, the following series of artificial defects were tested: dielectric-bounded single cavity (square, flat, narrow), electrode-bounded cavity (flat), multiple cavities, treeing initiated by a cavity, treeing initiated by a conductor. Also samples with surface discharges in air were tested.

Each series of discharges in solids consisted of Perspex™, PE and PVC samples containing a cylindrical cavity with specific dimensions. To account for the fact that cavities in actual dielectrics are not always regularly shaped with smooth surface, cavities with rough and irregular surface were studied (Figure 4). The surface with the roughness 3, 2 μm was simulated by mechanical working and controlled using a contact measuring probe. During the tests the specimens for internal discharges were placed in homogeneous field between Rogowski electrodes (Figure 5). The electrodes were partly covered with high-viscosity oil and partly embedded in polyester in order to prevent unwanted discharges at the electrode edges. Mechanical pressure on the electrodes ensured good contact with the dielectric. The setup was discharge free up to 9 kV/mm field strength, which made the study of discharges in the cavity possible [5]. To obtain cavities with trees these were aged beforehand. In the first 5 to 10 min of the test, treeing was initiated. To produce treeing discharges by a conductor, a needle/plane configuration was used with 100 μm radius of the point. Further, for these samples the test voltage was chosen such that treeing was initiated from the beginning. To obtain surface discharges, a metal electrode was placed on a dielectric surface of PE, Perspex or PVC.

The discharge analyzer records all above presented discharge quantities. A classic balanced discharge detection circuit was used, consisting of a detection bridge and a PD detector, Haefely Type 560 (Figure 6). The bandwidth has a lower limit of 40 kHz and an upper limit of 400 kHz. Using a transient recorder DataLab DL 919 the discharge signals and the test voltage were digitized with sampling frequency of 200 or 400 kHz and delivered to the computer. In this way the test voltage cycle was divided into 4000 or 8000 phase windows identical with φ_i in Figure 2. In order to synchronize the discharge signal with a 50 Hz time base, the transient recorder was triggered by an impulse delivered from the HV sine wave. To
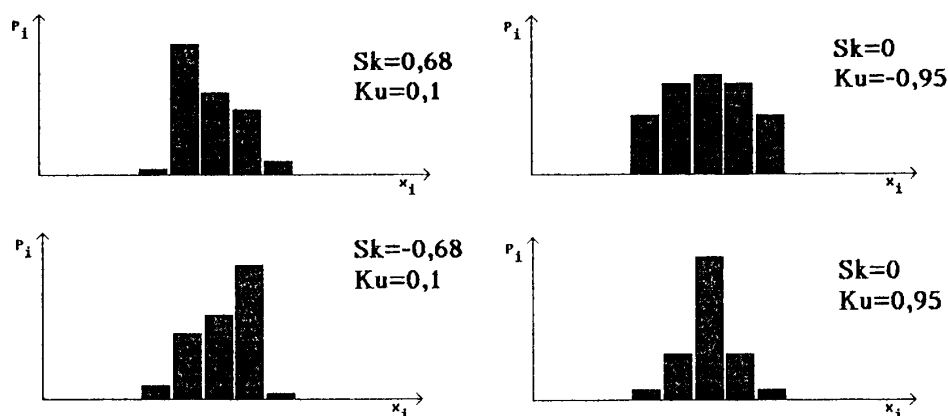
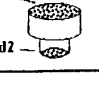Figure 3.   Typical distribution profiles and their skewness and kurtosis.

Figure 4.   Sample geometries.
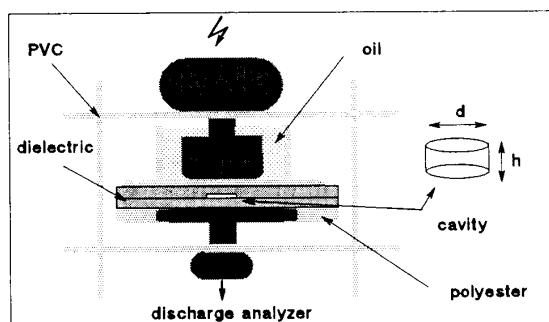
Figure 5.
Electrode configuration of samples with cavities.

Figure 6.
Block diagram of discharge analyzer.

identify the measured discharges in pC, a calibration of the system was made. To that effect, a known discharge

was injected in the sample, and a discharge resolution factor was calculated representing the smallest difference in discharge magnitude (> 1 pC) that can be detected. In order to prevent the registration of system noise as PD, all tests were subjected to a noise suppression of 10%. Therefore, only signals $> 10\%$ of the maximal discharge were analyzed.

For every half period the values of the inception voltage $U_{inc}(t)$ and the number of discharges $N_q(t)$ were processed. Further the distributions of phase angle quantities $H_{qn}(\varphi)$ and $H_n(\varphi)$ were calculated and stored in the computer. The analysis of $H_{qn}(\varphi)$ and $H_n(\varphi)$ distributions by means of the statistical operators was carried out after the measurement has been finished. All tests were subjected to a 20 min voltage test about 20% above the discharge inception voltage. Experience has shown [5,9] that a 20 min test period is sufficient to register the characteristics of a discharging cavity. The value of the voltage that was applied during the test was chosen at the level where no extinction of discharges was expected. The $H_{qn}(\varphi)$ and $H_n(\varphi)$ distributions of a 20 min test were investigated using the statistical operators. $H_{qn}(\varphi)$ was analyzed by Sk and mcc, whereas $H_n(\varphi)$ was analyzed by Ku. The operators Sk of $H_n(\varphi)$ and Ku of $H_{qn}(\varphi)$ were discarded as discriminators because no discriminative strength could be obtained. To register changes during the tests, the test time was divided into 2 min intervals. For each interval the distribution functions $H_{qn}(\varphi)$ with the Sk operators were analyzed.

4. TEST RESULTS

FIGURE 7 shows stylized examples of the typical time behavior of the inception voltage $U_{inc}(t)$ for discharges in solids. Depending on the sample, the magnitude of 100% for the $U_{inc}(t)$ was varied between 1.0 and 1.2× the peak value of the applied test voltage. The observation of $U_{inc}(t)$ provides a discrimination between three typical behaviors.

The dielectric-bounded single cavity and multiple cavities are characterized by typical increase of the discharge inception voltage $U_{inc}(t)$ in the first 5 to 10 min of the test (Figure 7(a)). During the tests, most changes in discharge patterns occurred in this time interval, whereas the discharge magnitude remained approximately the same. These changes can be explained by the creation of a (semi) conducting layer on the surface of the cavities, due to acid formation in the discharge process [9]. The (semi) conducting surfaces led to a changed electric field in the cavity, the voltage over the cavity decreases and the inception voltage rises accordingly.

For electrode-bounded cavities the difference in inception voltage in the positive and the negative half of the voltage cycle is interesting (Figure 7(b)). In the negative half of the voltage cycle the extinction occurs often, whereas in the positive one a stable inception voltage $U_{inc}(t)$ is reached after about 5 min [9]. During the positive half cycle the remnant charge at the dielectric surface, results in a larger supply of initiating electrons. In the negative half cycle initiating electrons have to be freed from the electrode or supplied by natural background radiation [16]. Treeing discharges are characterized by a strongly fluctuating inception voltage $U_{inc}(t)$ (Figure 7(c)).

Figure 8 shows stylized examples of the typical time behavior of the number of discharges $N_q(t)$ for tested samples. Depending on the sample, the magnitude of 100% for the $N_q(t)$ in most of the tests was between 8 and 16. The $N_q(t)$ quantity also provides a discrimination between characteristic behaviors. For single cavities and for multiple cavities a significant decrease of the number of discharges was observed (Figure 8(a)). This decrease follows the typical increase in inception voltage.

For treeing discharges an increasing number of discharges $N_q(t)$ is characteristic (Figure 8(b)). This is due to the formation of new hollow spaces allowing PD. A similar tendency is observed with surface discharges, where after 5 to 10 min the discharge number $N_q(t)$ increases, usually in the positive half of the voltage cycle (Figure 8(b)). These changes could well be explained by the creation of a (semi) conducting area at the surface due to discharge by-products. This results in larger electrode areas, in its turn causing a higher intensity of discharges.

Figures from 9 to 16 show typical comparisons between pulse count distribution $H_n(\varphi)$ and mean pulse height distribution $H_{qn}(\varphi)$, processed during 20 min test on ac voltage [17]. The comparison of these distributions shows that each defect is characterized by a specific shape of $H_{qn}(\varphi)$ and $H_n(\varphi)$ distributions, and that these differences are not easy to describe quantitatively. Therefore, these distributions were analyzed by means of the above described statistical operators.

In the first place the skewness Sk was calculated for ten $H_{qn}(\varphi)$ distributions in 2 min intervals. Three typical time functions of Sk are discriminated here (Figure 17). A single cavity and multiple cavities are characterized by strongly fluctuating Sk values (Figure 17(a)). Further, narrow cavities are characterized by zero or negative values of Sk on $H_{qn}(\varphi)$, whereas flat cavities are characterized by positive and higher values of Sk [15]. This dependence is better visible during the time that the discharges are stable [5].
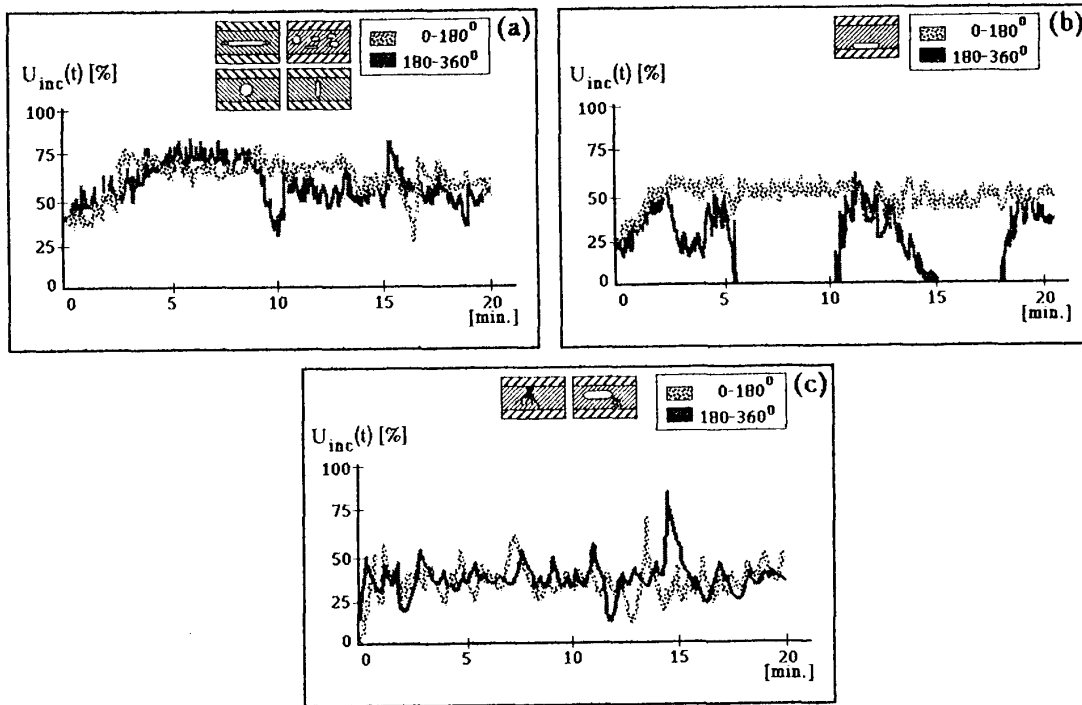
Figure 7.

Characteristic time dependence of the inception voltage $U_{inc}(t)$. (a) Dielectric-bounded cavities, (b) electrode-bounded cavities, (c) tree discharges.
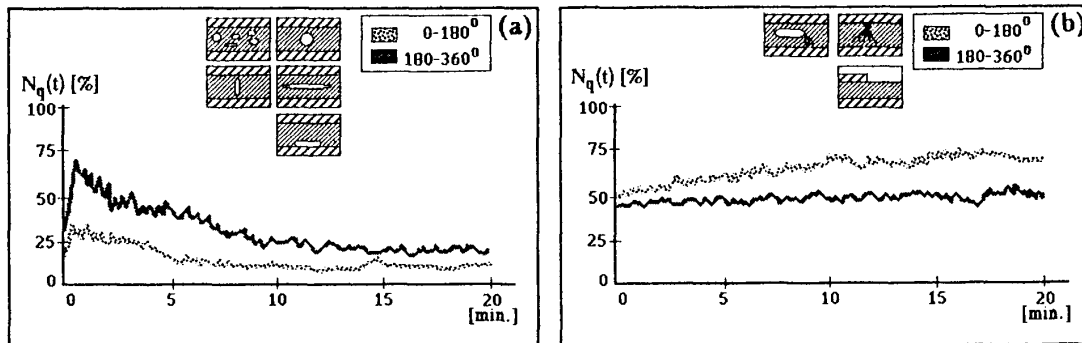

Figure 8.

Characteristic time dependence of the number of discharges $N_q(t)$. (a) Cavity discharges, (b) treeing discharges, surface discharges.

The time dependence of Sk of the $H_{qn}(\varphi)$ distribution of surface discharges is characterized by less fluctuating Sk values (Figure 17(b)). For treeing discharges initiated by a cavity it is characteristic that Sk is positive before treeing has started (Figure 17(c)). Afterwards Sk starts to fluctuate and becomes zero or negative [13]. For treeing at a conductor with treeing initiated from the beginning; Sk for $H_{qn}(\varphi)$ distributions is zero or negative (Figure 17(c)). This is better visible during the time, that the trees are growing.

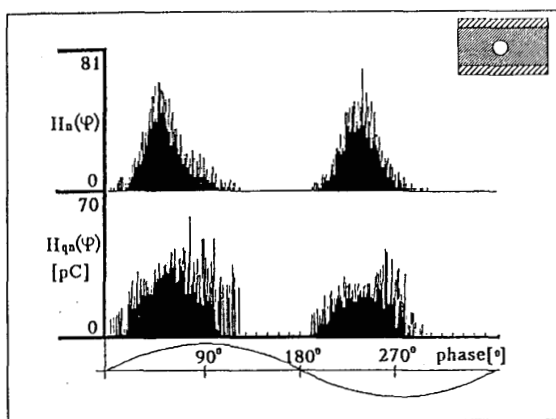In the second place the statistical operators Sk, Ku

Figure 9.
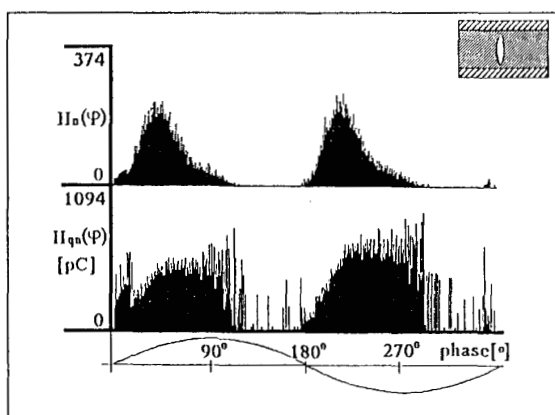$H_n(\varphi)$ and $H_{qn}(\varphi)$ characteristics for a square cavity.

Figure 10.
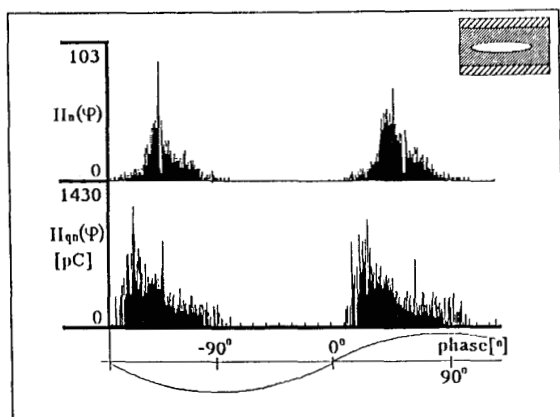$H_n(\varphi)$ and $H_{qn}(\varphi)$ characteristics for a narrow cavity.

Figure 11.
$H_n(\varphi)$ and $H_{qn}(\varphi)$ characteristics for flat cavity.

and mcc were calculated for all phase-position quantities
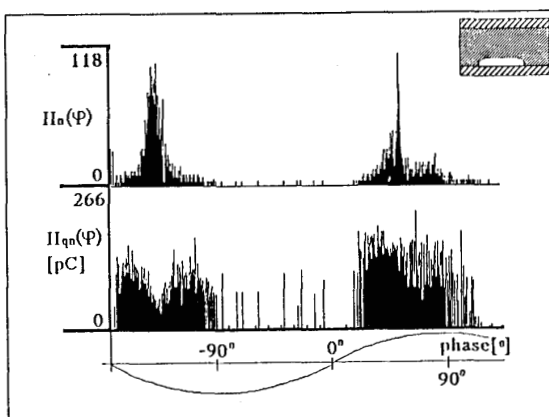

Figure 12.
$H_n(\varphi)$ and $H_{qn}(\varphi)$ characteristics for an electrode-bounded cavity.
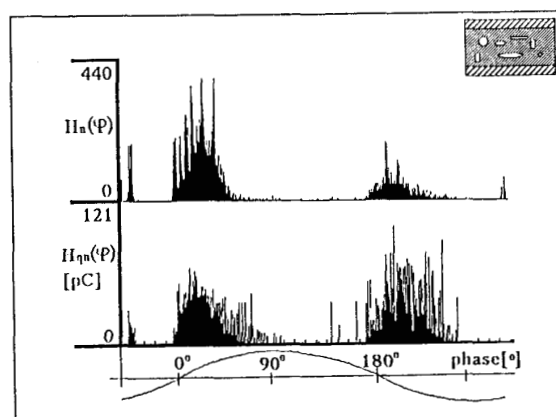

Figure 13.
$H_n(\varphi)$ and $H_{qn}(\varphi)$ characteristics for multiple cavities.

collected over the full 20 min. To determine if the values of a statistical operator obtained for a specific defect belong to the same population, series of 8 to 23 different tests were carried out for each type of defect. For each of the statistical operators, obtained with one type of defect, the mean value with 95% confidence interval was calculated (Figure 18). The following characteristics were observed for statistical operators:

Skewness Sk on $H_{qn}(\varphi)$

The values of the skewness are shown in Figure 18(a). The $H_{qn}(\varphi)$ distributions of dielectric-bounded cavities (square and flat) as well as those of electrode-bounded cavities are characterized by positive values of Sk. Further, $H_{qn}(\varphi)$ processed for multiple cavities is represented
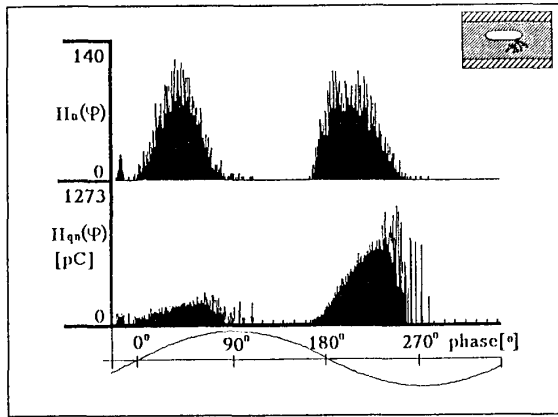
Figure 14.
$H_n(\varphi)$ and $H_{qn}(\varphi)$ characteristics for a cavity with treeing.
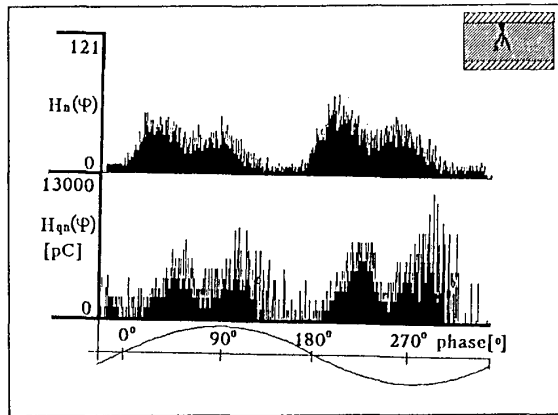

Figure 15.
$H_n(\varphi)$ and $H_{qn}(\varphi)$ characteristics for treeing on a conductor.

by positive Sk values too. In contrast, the $H_{qn}(\varphi)$ distributions of a narrow cavity, of surface discharges and of samples with treeing are characterized by zero or negative values of Sk.

Kurtosis Ku on $H_n(\varphi)$

The kurtosis Ku proved to be a good discriminator for multiple cavities and samples with treeing. Figure 18(b) shows that in the case of several discharge sites (samples with a tree or multiple cavities), the Ku value of the $H_n(\varphi)$ distribution is clearly negative. On the other hand, single discharge sites are characterized by positive Ku values of $H_n(\varphi)$ distributions. In contrast, surface discharges are characterized by negative Ku values for $H_n^-(\varphi)$ and positive Ku values for $H_n^+(\varphi)$.

Modified cross correlation mcc on $H_{qn}^+(\varphi)$ and $H_{qn}^-(\varphi)$
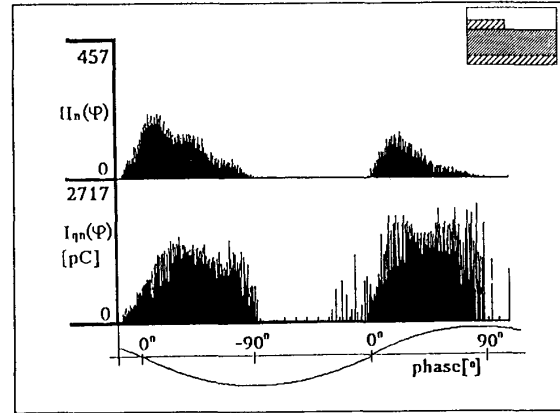

Figure 16.
$H_n(\varphi)$ and $H_{qn}(\varphi)$ characteristics for surface discharges in air.

Figure 18(c) shows the modified cross correlation mcc. This operator proved to be a good indicator for differences in shape between $H_{qn}^+(\varphi)$ and $H_{qn}^-(\varphi)$. It follows that the $H_{qn}(\varphi)$ distributions of an electrode-bounded cavity as well as cavity with treeing are characterized by lower values of mcc. In contrast the distributions $H_{qn}(\varphi)$ for dielectric-bounded cavities as well for treeing at a conductor and for surface discharges are characterized by higher values of mcc [9].

5. CONCLUSIONS

THE use of a multi-processing system for PD measurements provides a useful amount of discriminating data. The time functions inception voltage $U_{inc}(t)$ and the number of discharges $N_q(t)$ were processed. $H_{qn}(\varphi)$ and $H_n(\varphi)$ distributions of discharges were analyzed by means of statistical operators. An important improvement in characterizing discharges was shown by using operators, which represent a statistical analysis of the phase-position distributions. Examples of such operators are skewness Sk, kurtosis Ku and the modified cross-correlation factor mcc. It has been shown that the statistical operators for all these distributions give a more efficient discrimination between different discharge sources. The following conclusions can be drawn from the results of this investigation:

1. The inception voltage $U_{inc}(t)$ shows an increasing time dependence in the case of discharges in dielectric-bounded and electrode-bounded cavities [9].
2. Surface discharges and treeing discharges are distinguished from other sources by the increase of the number of discharges $N_q(t)$ with time, whereas with cavity discharges a decrease of $N_q(t)$ is characteristic.
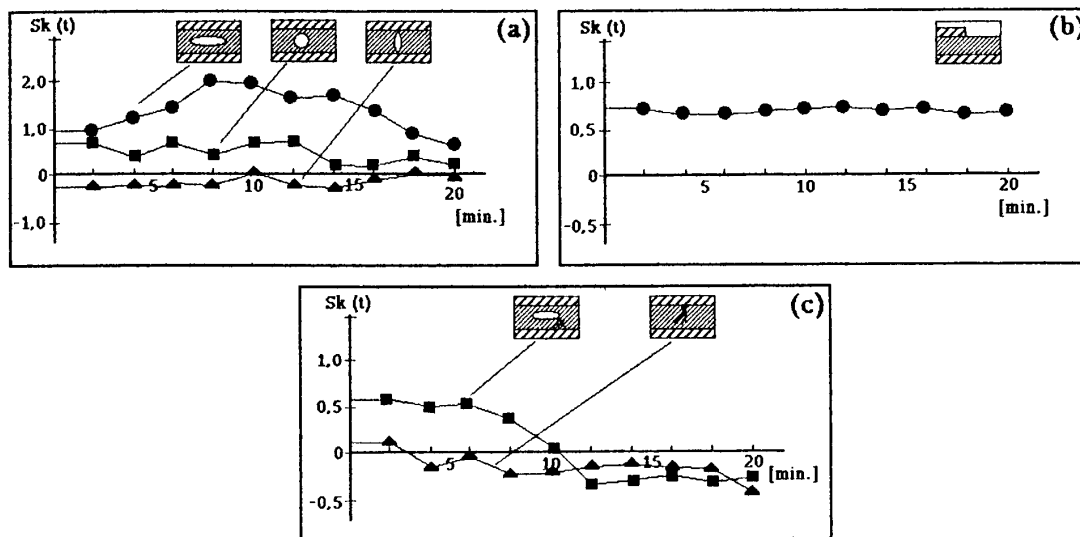
Figure 17.

Characteristic time dependence of skewness Sk on $H_{qn}(\varphi)$ distributions. (a) Cavity discharges, (b) surface discharges, (c) tree discharges.

3. A narrow cavity, samples with trees as well as surface discharges, are characterized by zero or negative values of the skewness Sk of $H_{qn}(\varphi)$ distributions.

4. Both a cavity with trees as well as a electrode-bounded cavity are characterized by a distinct difference between the distribution of $H_{qn}^{+}(\varphi)$ and $H_{qn}^{-}(\varphi)$. Therefore the modified cross-correlation factor mcc is low, whereas in other defects more symmetry is found and the mcc is much higher.

5. Samples with trees and multiple cavities show (in contrast to other defects) equal shapes of the $H_{n}(\varphi)$ distribution. This results in negative values for the kurtosis Ku of these distributions.

6. Surface discharges are characterized by negative Ku values for $H_{n}^{-}(\varphi)$ distributions and positive Ku values for $H_{n}^{+}(\varphi)$.

7. The time function of the Sk of $H_{qn}(\varphi)$ is characterized by less fluctuating values for surface discharges, whereas during the growth of trees it is characterized by negative values.

The above mentioned characteristics may prove to be useful for the development a system for the diagnose of defects in insulating constructions.

REFERENCES

[1] F. H. Kreuger, *Partial Discharge Detection in HV Equipment*, Butterworths, England, 1989.

[2] K. Möller, "Tendenzen der Isolierstoffforschung", E und M, Vol. 98, pp. 198–206, 6/1989.

[3] J. D. Gassaway, P. B. Jacob and C. A. Vassiliadis "Computer-aided PD Measurement and Recognition", Proceedings of the 5th Int. Symp. on HV, paper 41.03, Braunschweig 1987.

[4] T. Okamoto and T. Tanaka "Novel PD-measurement Computer Aided Measurement System", Transaction on Electrical Insulation, Vol. 21, pp. 1015–1019 December 1986.

[5] E. Gulski and F. H. Kreuger "Digital Computer System for Measurement of Partial Discharges in Insulation Structures", Proceedings of the 3rd Conf. on Cond. and Break. in Sol. Dielect., pp. 582–586, Trondheim, 1989.

[6] H.-G. Kranz and R. Krump "The Ability of Self-operating Expert Systems for Statistical Partial Discharge Analysis of GIS-Test Signals", 6th Int. Symp. on HV, paper 22.13, New Orleans, 1989.

[7] F. H. Kreuger and E. Gulski "Simultane Erfassung und Verarbeitung von Teilentladungs-Kenngrössen zur Beurteilung elektrischer Isolierungen", Technisches Messen, Vol. 55, pp. 17–22, 1/1988.

[8] F. H. Kreuger and E. Gulski "Automatisiertes Meßsystem zur Erfassung von Teilentladungs-Kenngrössen für die Beurteilung elektrischer Isolierungen", Technisches Messen, Vol. 56, pp. 124–129, 3/1989.
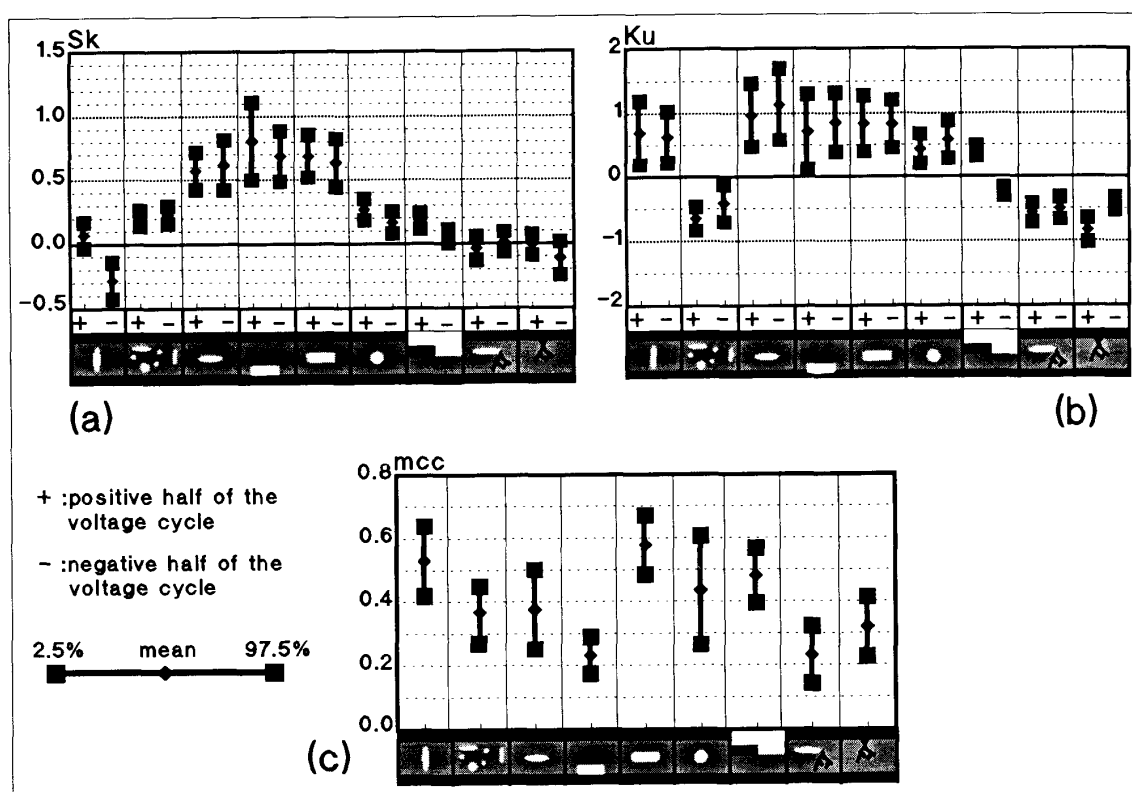
Figure 18.

Statistical operators processed for discharge sources. (a) Skewness Sk of $H_{qn}(\varphi)$ distributions, (b) Kurtosis Ku of $H_n(\varphi)$ distributions, (c) Modified cross-correlation factor mcc of $H_{qn}(\varphi)$ distributions.

[9] E. Gulski, P. H. F. Morshuis and F. H. Kreuger "Automized Recognition of Partial Discharges in Cavities", Japanese Journal of Applied Physics, Vol. 29, pp. 7–13, 7/1990.

[10] S. Karkkainen, Internal Partial Discharge Pulse Distributions, Physical Mechanisms and Effects on Insulation, Thesis Institute of Technology Helsinki, 1976.

[11] E. Neudert and R. Porzel, "Ein oscillografisches Verfahren zum Beurteilung von Teilentladungen", Elektrie, Vol. 22, pp. 360–362, 9/1968.

[12] A. Kelen, "The Functional Testing of HV Generator Stator Insulation", CIGRE paper 15–03, Appendix A, 1976.

[13] T. Tanaka and T. Okamoto, "Analysis of q-n and ϕ-q Characteristics of Partial Discharge in Several Electrode Systems", Proceedings of the IEEE Int. Symp. Electrical Insulation, pp. 190–194, New York, 1980.

[14] W. L. Hays, Statistics, pp. 166–167, Tokyo, Holt Rinehart and Winston, 1981.

[15] T. Tanaka and T. Okamoto, "An Advanced Partial Discharge Measurement Method Sensitive to the Shape of a Void", in Proceedings of the Inter. Conf. on Large HV Electric System, paper 15–02, Paris, 1988.

[16] P. H. F. Morshuis, "New Insight into Discharge in Voids", Proceedings of the Meeting of the Dielectrics Society, p. 37, Canterbury, 1990.

[17] E. Gulski, "Computer-aided Analysis of Discharge Types", Proceedings of the Meeting of the Dielectrics Society, p. 38, Canterbury, 1990.